Since January 2020 Elsevier has created a COVID-19 resource centre with free information in English and Mandarin on the novel coronavirus COVID-19. The COVID-19 resource centre is hosted on Elsevier Connect, the company's public news and information website.

Journal of Virological Methods 193 (2013) 639–646

Contents lists available at ScienceDirect

Journal of Virological Methods

journal homepage: www.elsevier.com/locate/jviromet

The replication of a mouse adapted SARS-CoV in a mouse cell line stably expressing the murine SARS-CoV receptor mACE2 efficiently induces the expression of proinflammatory cytokines

Jose A. Regla-Nava[a], Jose M. Jimenez-Guardeño[a], Jose L. Nieto-Torres[a], Thomas M. Gallagher[b], Luis Enjuanes[a,*], Marta L. DeDiego[a]

[a] Department of Molecular and Cell Biology, Centro Nacional de Biotecnología (CNB-CSIC), Darwin 3, Campus Universidad Autónoma de Madrid, 28049 Madrid, Spain
[b] Department of Microbiology and Immunology, Loyola University Medical Center, 2160 South First Avenue, Maywood, IL 60153, USA

Article history:
Received 7 March 2013
Received in revised form 10 July 2013
Accepted 15 July 2013
Available online 1 August 2013

Keywords:
SARS
Coronavirus
Mouse adapted
Stably transformed murine cells
SARS-CoV receptor ACE2
Proinflammatory cytokines

A B S T R A C T

Infection of conventional mice with a mouse adapted (MA15) severe acute respiratory syndrome (SARS) coronavirus (CoV) reproduces many aspects of human SARS such as pathological changes in lung, viremia, neutrophilia, and lethality. However, established mouse cell lines highly susceptible to mouse-adapted SARS-CoV infection are not available. In this work, efficiently transfectable mouse cell lines stably expressing the murine SARS-CoV receptor angiotensin converting enzyme 2 (ACE2) have been generated. These cells yielded high SARS-CoV-MA15 titers and also served as excellent tools for plaque assays. In addition, in these cell lines, SARS-CoV-MA15 induced the expression of proinflammatory cytokines and IFN-β, mimicking what has been observed in experimental animal models infected with SARS-CoV and SARS patients. These cell lines are valuable tools to perform in vitro studies in a mouse cell system that reflects the species used for in vivo studies of SARS-CoV-MA15 pathogenesis.

1. Introduction

Severe acute respiratory syndrome coronavirus (SARS-CoV) is an enveloped plus-strand RNA virus of the *Coronaviridae* family, genus β, within the *Nidovirales* order (de Groot et al., 2012; Enjuanes et al., 2008). SARS-CoV was first detected in late 2002 in Guangdong province, China and spread to more than 30 countries in a few months, causing 8000 infections and 800 deaths (Drosten et al., 2003; Fouchier et al., 2003; Ksiazek et al., 2003; Kuiken et al., 2003; Marra et al., 2003; Peiris et al., 2003; Rota et al., 2003). The spread of the virus was ultimately controlled by the isolation of infected individuals, and the WHO declared the end of the SARS epidemic in July 2003. However, SARS-like coronaviruses remain and are circulating in bats all over the world, making virus reemergence a realistic possibility (Lau et al., 2005; Li et al., 2005; Woo et al., 2006).

Coronaviruses encode two overlapping open reading frames (ORFs 1a and 1b) that are translated into two polyproteins which are processed by two viral proteases to yield 16 non-structural replicase proteins (Ziebuhr et al., 2000). These proteins are involved in genome replication and transcription of subgenomic mRNAs encoding the structural proteins nucleocapsid (N), envelope (E), membrane (M) and spike (S), as well as a set of CoV species-specific proteins. The spike protein is localized at the surface of the virion, and is responsible for the attachment to the cellular receptor, and for virus-cell membrane fusion, to facilitate virus entry (Gallagher and Buchmeier, 2001). The cellular receptor for SARS-CoV is the angiontesin convertin enzyme 2 (ACE2) (Li et al., 2003; Wong et al., 2004), although the glycoprotein CD209L (L-SIGN) may also be used as a weaker alternative receptor (Jeffers et al., 2004).

SARS-CoV infects many experimental animals such as mice, ferrets, cats, hamsters and non-human primates (cynomolgus and rhesus macaques, African green monkeys and marmosets) (Roberts et al., 2008; Subbarao and Roberts, 2006). However, none of the infection models completely reproduce human clinical disease and pathological findings. To overcome these limitations, SARS-CoV was adapted to grow in mice by passing the virus in lung for 10, 15, or 25 times (Day et al., 2009; Nagata et al., 2008; Roberts et al.,

* Corresponding author at: Department of Molecular and Cell Biology, Centro Nacional de Biotecnología (CNB-CSIC), Darwin 3, Cantoblanco, 28049 Madrid, Spain. Tel.: +34 915854555; fax: +34 915854506.
E-mail address: L.Enjuanes@cnb.csic.es (L. Enjuanes).

0166-0934/$ – see front matter © 2013 Elsevier B.V. All rights reserved.
http://dx.doi.org/10.1016/j.jviromet.2013.07.039

2007). Infection of Balb/c mice with the resulting mouse adapted (MA) viruses reproduced many aspects of human SARS, including pathological changes in the lung, viremia, neutrophilia, and lethality (Day et al., 2009; Nagata et al., 2008; Roberts et al., 2007). This inbred mouse model of human SARS disease has many advantages compared to the other animal models, such as small animal size, low cost, availability of the animals, the possibility to genetically manipulate the host animals (i.e. to develop gene knock-outs and knock-ins), and the availability of immunological and molecular biology reagents specific to the host animals.

Coronaviruses generally do not induce a high interferon response (Frieman et al., 2008). At least two mechanisms have been proposed to explain the low levels of type I interferon (IFN-α and -β) during coronavirus infections: the sequestering of viral RNA in double membrane vesicles (Gosert et al., 2002; Knoops et al., 2008), which prevents or reduces recognition by pattern recognition receptors (PRRs); and the expression of viral proteins that antagonize the innate response. In fact, SARS-CoV proteins nsp1, nsp3, 3b, 6, M and N act as interferon antagonists (Devaraj et al., 2007; Frieman et al., 2007; Kopecky-Bromberg et al., 2007; Narayanan et al., 2008; Siu et al., 2009; Sun et al., 2012; Wathelet et al., 2007). However, even with these viral strategies of defensive evasion and offensive antagonism of interferons, there are well-described host proinflammatory responses to in vivo SARS-CoV infections. Inflammatory mediators such as interleukin (IL)-1, -6, and -8, CXCL10/interferon-inducible protein (IP)-10, CCL2/monocyte chemoattractant protein (MCP)-1, CCL5/protein regulated and normal T expressed and secreted (RANTES), and CXCL9/monokine induced by interferon gamma (MIG) have been recognized in lungs of patients affected by SARS (Cameron et al., 2007; Huang et al., 2005; Jiang et al., 2005; Reghunathan et al., 2005; Tang et al., 2005; Wong et al., 2003; Zhang et al., 2004). Upregulation of genes mediating inflammation has also been described after infection with SARS-CoV in different animal models such as cynomolgus macaques and African green monkeys (de Lang et al., 2007; Smits et al., 2010, 2011) and mice (Baas et al., 2008). Accordingly, the expression of several proinflammatory genes is considered to be a strong correlate of SARS-CoV induced pathology.

Several established cell lines from different species, including monkey cells Vero E6, MA104 and FRhK-4, human cells Caco-2, CL-14, LoVo and Huh-7, pig cells PK-15, POEK and PS, and mink cells Mv 1 Lu (Chan et al., 2004; Cinatl et al., 2004; Hattermann et al., 2005; Mossel et al., 2005; Ng et al., 2003) are susceptible to SARS-CoV infection. However, not all of these cell lines possess the full complement of genes encoding innate immune signaling and response factors, and as such, some of the cell lines are not suitable for evaluating the innate host response to SARS-CoV. Mouse DBT cells have been transfected with human or civet SARS-CoV receptor ACE2 (Becker et al., 2008; Sheahan et al., 2008a,b). However, as far as we know, the susceptibility of these cell lines to a mouse adapted SARS-CoV has not been determined. In addition, mouse cell lines have never been stably transfected with the mouse ACE2, which is the natural receptor used by the mouse adapted SARS-CoV.

In this work, we established mouse cell lines stably expressing the murine SARS-CoV receptor ACE2 (Li et al., 2003; Wong et al., 2004). These cell lines were highly susceptible to mouse adapted SARS-CoV infection and were also transfectable with high efficiency. Using these cell lines, we demonstrated that a mouse adapted SARS-CoV (SARS-CoV-MA15) induced the expression of genes leading to inflammation, as shown in SARS patients and experimental animal models infected with SARS-CoV. In addition, SARS-CoV-MA15 induced a weak IFN-β response, as generally shown in coronavirus infections, preventing the robust production of type I IFNs. These mouse cell lines are valuable tools to perform in vitro studies that could be further developed in the species-homologous SARS mouse models.

2. Materials and methods

2.1. Cells

Delayed brain tumor (DBT) cells were originally obtained from an intracerebral tumor induced in an adult BALB/c mouse by intracerebral injection of Rous sarcoma virus (Kumanishi, 1967). The African green monkey kidney-derived Vero E6 cells were kindly provided by Snijder (University of Leiden, The Netherlands). Cells were cultured in Dulbecco's modified Eagle's medium (DMEM, GIBCO) supplemented with 25 mM HEPES, 10% fetal bovine serum (FBS, Biowhittaker), and 1% non-essential amino acids (SIGMA) and incubated in a 5% CO_2 atmosphere, at 37 °C.

2.2. Plasmids

The plasmid pcDNA3.1 encoding the murine ACE2 gene (GeneBank sequence NM_001130513.1) fused to 5′ myc tag codons (pcDNA3.1-myc-mACE2), and a gene providing geneticin (G418) resistance in prokaryotic and eukaryotic cells, was kindly provided by Farzan (Harvard Medical School, USA) (Li et al., 2004). SARS-CoV full-length cDNAs encoding the Urbani strain or the mouse adapted strain (MA15) were assembled in bacterial artificial chromosomes (BACs) under the control of the cytomegalovirus (CMV) immediate-early promoter to allow the expression of the viral RNA in the nucleus by cellular RNA polymerase II. At the 3′ end, these cDNAs were flanked by a 25-bp poly(A) tail, followed by the hepatitis delta virus ribozyme and the bovine growth hormone and termination and polyadenylation sequences, to generate a correct 3′ end (Almazan et al., 2006, 2000).

2.3. Viruses

SARS-CoV-Urbani and SARS-CoV-MA15 viruses (Roberts et al., 2007) were rescued from infectious cDNA clones generated (Almazan et al., 2006; Fett et al., 2013). To recover infectious viruses, BHK cells were grown to 95% confluence in a 25-cm^2 flask and transfected with the cDNA clones by using Lipofectamine 2000 (Invitrogen) according to the manufacturer's specifications. At 6 h posttransfection (hpt), cells were trypsinized, plated over a confluent monolayer of Vero E6 cells grown in a 25-cm^2 flask, and incubated at 37 °C for 72 h. After one passage in Vero E6 cells, the recovered viruses were cloned by three rounds of plaque purification. All work with infectious viruses was performed in biosafety level (BSL) 3 plus facilities. All personnel were equipped with positive-pressure air purifying respirators (3 M HEPA AirMate, St. Paul, MN).

2.4. Generation of DBT cells stably expressing mACE2

To transfect DBT-mACE2 with high efficiency, 3×10^5 DBT-mACE2 cells were transfected using the program EN-158 of Amaxa 4D-Nucleofector and 1 μg of the linearized plasmid pcDNA3.1-myc-mACE2 in buffer SG (Lonza). Nucleofected cells were seeded on 24-well plates. After nucleofection, cells were incubated for 10 min at room temperature (RT), and then the cells were added to DMEM (GIBCO) supplemented with 25 mM HEPES, 10% fetal bovine serum (FBS, Biowhittaker) and 1% non-essential amino acids (SIGMA) and incubated at 37 °C. 24 h post-nucleofection, G418 was added to the culture medium, to a final concentration of 800 μg/ml, to select for geneticin resistance. The selective medium was changed every 3–4 days for 2 weeks, and the cells were cloned three times by limiting dilution (1 cell/well) in the presence of G418

(800 μg/ml). Subsequently, ten clones of DBT-mACE2 were amplified in the presence of 800 μg/ml of G418.

2.5. Transfection of DBT-mACE2 clones

To analyze the efficiency of transfection, DBT-mACE2 cells were nucleofected as described above, using a GFP-encoding plasmid. 24 h post nucleofection GFP expression was analyzed by fluorescence activated cell sorting (FACS). DBT-mACE2 cells were transfected with an efficiency higher than 90%.

2.6. Indirect immunofluorescence microscopy

To detect viral N proteins and the myc tag fused to mACE2, DBT-mACE2 cells were grown to 80% confluence on glass coverslips and infected with rSARS-CoV-MA15 at a moi of 0.1. At 24 hpi, media were removed and cells were washed twice with PBS and fixed and permeabilized with ice-cold 100% methanol for 20 min at −20 °C or with 4% paraformaldehyde in phosphate buffered saline (PBS) for 30 min at room temperature, in the case of non-permeabilized cells. Primary antibody incubations were performed in PBS containing 10% FBS for 90 min at room temperature. The mouse mAb SA46-4 specific for N protein, kindly provided by Fang (South Dakota State University, Brookings, USA) (dilution 1:500), and a mouse anti-myc (dilution 1:500, Millipore, Ref. 05-724), were used. Coverslips were washed two times with PBS between primary and secondary antibody incubations. Secondary antibodies (Invitrogen) were Alexa 488 (for detection of N protein) or Alexa 594 (for detection of myc tag) conjugates and were incubated for 45 min at room temperature at 1:500 dilutions in PBS containing 10% FBS. Nuclei were stained using DAPI (dilution 1:200, Sigma). Coverslips were mounted in Prolong Gold anti-fade reagent (Invitrogen) and examined on a Leica SP5 confocal microscope (Leica Microsystems). The percentage of mACE2 and viral N-positive cells were calculated by analyzing 10 random fields, each one containing at least 30 cells.

2.7. Virus production in different DBT-mACE2 clones

DBT-mACE2 clones grown to densities of 3.0×10^5 cells/cm^2 were infected at a moi of 0.1 with SARS-CoV-MA15 or SARS-CoV-Urbani. Culture supernatants were collected at 72 hpi, and virus titers were determined in Vero E6 cells as previously described (DeDiego et al., 2007).

To analyze the effect of the moi on virus production, DBT-mACE2 clone 6 cells, which supported the highest viral titers, were infected at mois ranging from 0.0001 to 1 pfu per cell with the rSARS-CoV-MA15 virus. Culture supernatants were collected at the indicated times post-infection and titrated on Vero E6 cells.

To determine the effect of cell density on virus production, DBT-mACE2 clone 6 cells at different cell densities were infected at a moi of 0.1. Culture supernatants were collected at 72 hpi and titrated in Vero E6 cells.

2.8. Virus titration in DBT-mACE2 cells

DBT-mACE2 clone 6 cells at a cell density of 2.5×10^5 cells/cm^2 were infected with SARS-CoV-MA15. Cell cultures were incubated at 37 °C for 60 min for virus adsorption and then overlaid with DMEM containing 0.6% low melting agarose and 4% FBS. 48 hpi, cells were fixed with 10% formaldehyde in PBS and stained with a solution containing 0.1% (w/v) crystal violet and 20% methanol.

2.9. Expression of inflammation-related cytokines and IFN-β and -γ in rSARS-CoV-MA15 infected cells

DBT-mACE2 clone 6 cells were infected with rSARS-CoV at a moi of 0.1. Total RNAs from DBT-mACE2 infected cells were extracted at 48 hpi using the Qiagen RNeasy kit according to the manufacturer's instructions. Quantitative reverse transcription-polymerase chain reaction (qRT-PCR) reactions were performed at 37 °C for 2 h with a High Capacity cDNA transcription kit (Applied Biosystems) using 100 ng of total RNA and random hexamer oligonucleotides. Cellular gene expressions were analyzed using TaqMan gene expression assays (Applied Biosystems) specific for *Mus musculus* genes (Table 1). Data were acquired with an ABI PRISM 7000 sequence detection system (Applied Biosystems) and analyzed with ABI PRISM 7000 SDS version 1.0 software. Gene expression in mock-infected cells and rSARS-CoV-MA15-infected cells was compared. Quantification was achieved using the $2 - \Delta\Delta$Ct method, which analyzes relative changes in gene expression in qPCR experiments (Livak and Schmittgen, 2001). The results of three independent experiments were analyzed. DBT-mACE2 clone 6 cells were infected at a moi of 0.1 and cell extracts in lysis buffer (1% NP-40, 50 mM Tris–HCl, pH 7.6, 2 mM NaCl, 2 mM EDTA and protease inhibitors) were prepared at 48 hpi. Cell extracts were diluted 1:5 in assay buffer (Millipore). The expression of mouse CXCL10/IP-10 and CXCL2/macrophage inflammatory protein 2 (MIP-2) was evaluated with the Luminex technology and a mouse cytokine antibody bead kit (Milliplex map kit; Millipore), following the manufacturer's instructions. Data were collected from three independent infections.

3. Results

3.1. Generation of mouse DBT cells expressing the SARS-CoV receptor mACE2

To generate a mouse cell line susceptible to SARS-CoV infection, DBT cells were nucleofected with a plasmid encoding the SARS-CoV receptor mACE2 fused N-terminally to a myc tag (myc-mACE2) along with an antibiotic resistance marker. Transfected cells were selected by using geneticin (G418). Ten independently-derived cell clones were generated. mACE2 expression in the different clones was analyzed by immunofluorescence using an antibody specific for the myc tag. The ten selected clones showed high mACE2 expression in more than 70% of the cells (Fig. 1A and B). The myc-mACE2 expression was stable for at least 20 passages in tissue culture (data not shown). Myc-mACE2 was detected in the plasma membrane even in non-permeabilized cells, confirming that mACE2 is present at the cell surface. As expected, myc-mACE2 was undetectable in untransfected DBT cells (Fig. 1A and B). To determine whether the DBT-mACE2 clones were easily transfected with plasmid DNAs (a useful method for future studies), the cells were nucleofected with a plasmid encoding green fluorescent protein (GFP). Interestingly, the efficiency of DBT-mACE2 nucleofection was greater than 90% (data not shown).

3.2. Susceptibility of DBT-mACE2 to SARS-CoV infection

To determine whether the DBT-mACE2 cells were susceptible to SARS-CoV, the 10 selected clones, untransfected DBT cells, and positive-control Vero E6 cells were infected with the mouse adapted SARS-CoV-MA15 strain at a moi of 0.1. No infectious virus was recovered from untransfected DBT cells at 72 hpi (Fig. 2A). Interestingly, in transfected cells, all DBT-mACE2 clones showed high viral titers at 72 hpi, ranging from 5.0×10^6 to 1.2×10^7 pfu/ml, respectively. DBT-mACE2 clones 1 and 6 produced the highest virus

Table 1
Taqman assays used to analyze the expression of cellular genes by quantitative RT-PCR.

Gene name	Taqman assay[a]	Description
TNF	Mm00443258-m1	Tumor necrosis factor
IL-1α	Mm00439620-m1	Interleukin 1α
IL-1β	Mm01336189-m1	Interleukin 1β
IL-6	Mm00446190-m1	Interleukin 6
CCL2/MCP-1	Mm00441242-m1	Monocyte chemotactic protein 1
CCL5/RANTES	Mm01302428-m1	Regulated upon activation, normal T-cell expressed, and secreted
CXCL1/NAP-3	Mm04207460-m1	Neutrophil activating protein 3
CXCL2/MIP-2	Mm00436450-m1	Macrophage inflammatory protein 2
CXCL10/IP-10	Mm00445235-m1	Interferon inducible protein 10
IFN-β	Mm00439552-s1	Interferon β
IFN-γ	Mm01168134-m1	Interferon γ
18S	Mm03928990-g1	Ribosomic RNA 18S

[a] Mm, means Mus musculus.

outputs (9.2×10^6 and 1.2×10^7 pfu/ml), which were as high as those obtained in Vero E6 cells (Fig. 2A).

To analyze whether DBT-mACE2 cells were also susceptible to a non-mouse adapted SARS-CoV, the clone 6 of DBT-mACE2 cells, producing the highest SARS-CoV-MA15 titers, untransfected DBT cells and Vero E6 cells were infected with SARS-CoV-Urbani.

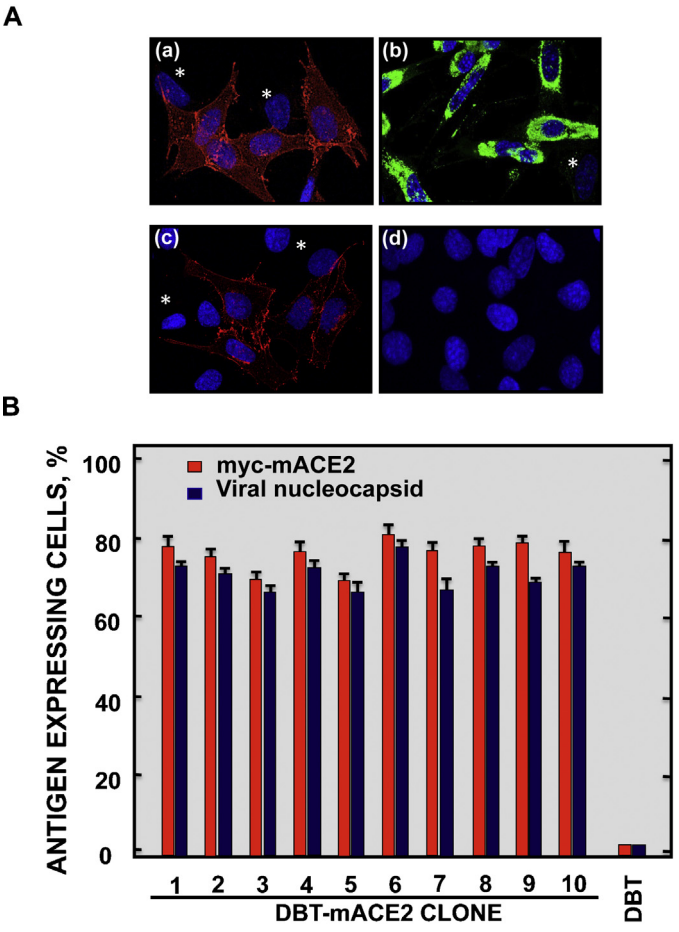

Fig. 1. Expression of myc-mACE2 and viral nucleoprotein in DBT-mACE2-infected clones. (A) Untransformed DBT and DBT-mACE2 cells were infected at a moi of 0.1 with rSARS-CoV-MA15. Myc-mACE2 and viral nucleoprotein expression was analyzed by indirect immunofluorescence using specific myc and nucleoprotein antibodies followed by A549 and A488-conjugated secondary mouse antibodies. Asterisks indicate cells that do not express myc-mACE2 or viral nucleoprotein, as controls. (a) myc-mACE2 in permeabilized cells, (b) viral nucleoprotein in permeabilized cells, (c) myc-mACE2 in non-permeabilized cells and (d) myc-mACE2 and nucleoprotein in untransformed DBT cells. (B) The percentage of myc-mACE2 positive and viral N protein-positive cells was calculated by analyzing 10 random fields, each one containing 30 cells.

Infectious viruses were also recovered in DBT-mACE2 cells, although with titers more than 10^3-fold lower than those for SARS-CoV-MA15 (Fig. 2B). In contrast, no infectious virus was recovered from untransfected DBT cells. SARS-CoV-Urbani and MA15 virus titers in Vero E6 cells were similar for both viruses (Fig. 2A and B).

To identify conditions for optimal virus production, moi and cell density parameters were varied. Firstly, DBT-mACE2 clone 6 cells were infected with SARS-CoV-MA15 at mois ranging from 0.0001 to 1. Virus titers were determined at 0, 4, 24, 48 and 72 hpi (Fig. 3). The highest viral titer (>10^7 pfu/ml) was obtained at moi of 0.1. Virus

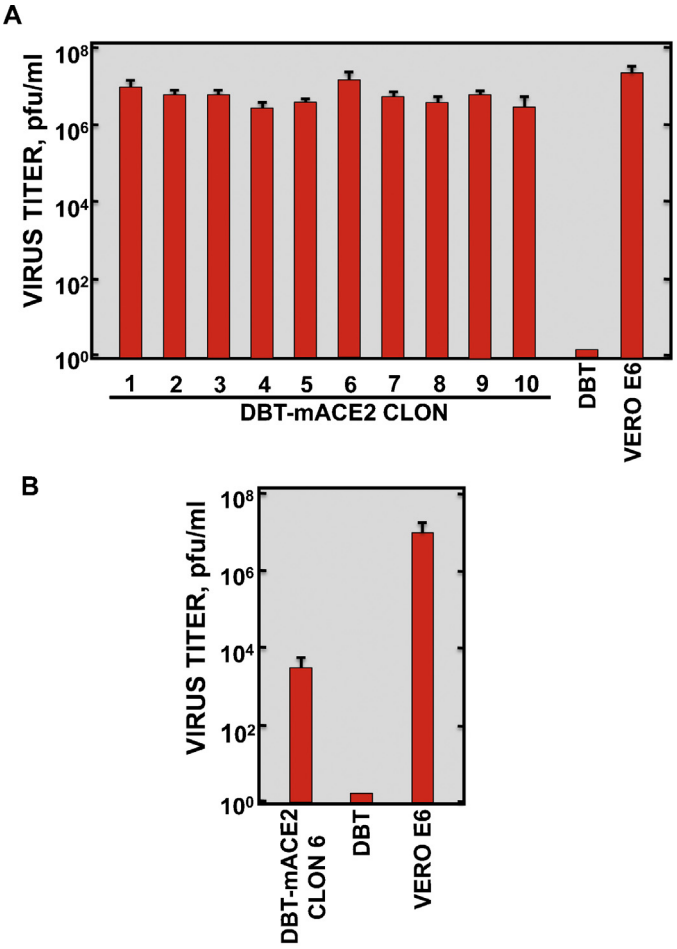

Fig. 2. SARS-CoV production in DBT-mACE2 cell clones. Cells were infected at a moi of 0.1 with rSARS-CoV-MA15 (A) or rSARS-CoV-Urbani. (B) Viral titers in cell supernatants at 72 hpi were measured using a plaque assay on Vero E6 cells. Error bars represent standard deviations of the mean from three experiments.

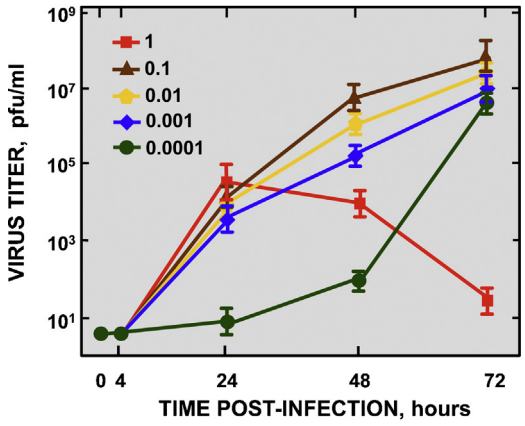

Fig. 3. Effect of moi on the growth kinetics of SARS-CoV-MA15 in DBT-mACE2 clone 6 cells. DBT-mACE2 clone 6 cells were infected at the indicated input mois. Viral titers in cell supernatants at the indicated times post-infection were measured by plaque assay on Vero E6 cells. Error bars represent standard deviations of the mean from three experiments.

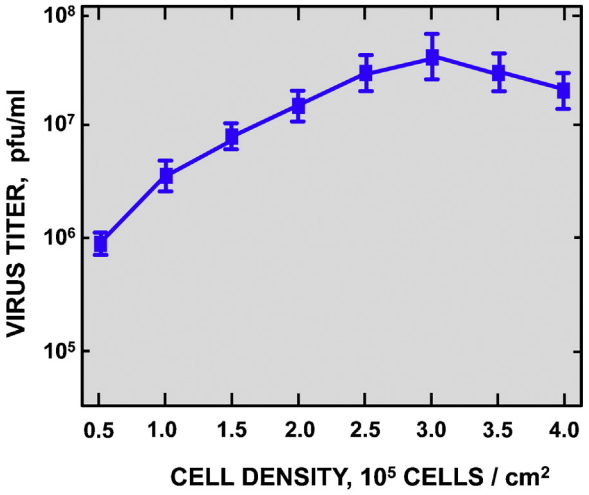

Fig. 4. Effect of cell density on the growth of SARS-CoV-MA15 in DBT-mACE2 clone 6 cells. DBT-mACE2 clone 6 cells were seeded at different cell densities and infected at a moi of 0.1. Viral titers in cell supernatants at 72 hpi were measured by plaque assay on Vero E6 cells. Error bars represent standard deviations of the mean from three experiments.

titers in cells infected with a moi of 1 rapidly decreased after 24 hpi, probably due to extensive cell death. Indeed, considerable cytopathic effect (CPE) was observed by microscopy. DBT-mACE2 clone 6 cells were also infected at cells densities ranging from 0.5×10^5 and 4×10^5 cells/cm^2, at the optimal moi of 0.1, and virus titers were determined at 72 hpi. The highest viral titers (>10^7 pfu/ml) were observed at a cell density of 3×10^5 cells/cm^2 (Fig. 4).

To determine the percentage of infected cells, untransfected DBT cells, and DBT-mACE2 clones were infected with SARS-CoV-MA15, and analyzed by immunofluorescence with an antibody specific for the viral N protein (Fig. 1A and B). The percentage of infected cells, detected by the presence of N protein, was higher than 70% in all the DBT-mACE2 transfected clones.

SARS-CoV infection caused CPE in DBT-mACE2 cells. At input mois of 0.1, cell rounding and detachment was evident at 48 hpi, being almost total at 72 hpi. Control uninfected cells showed no morphological changes (Fig. 5A). In fact, SARS-CoV-MA15 formed

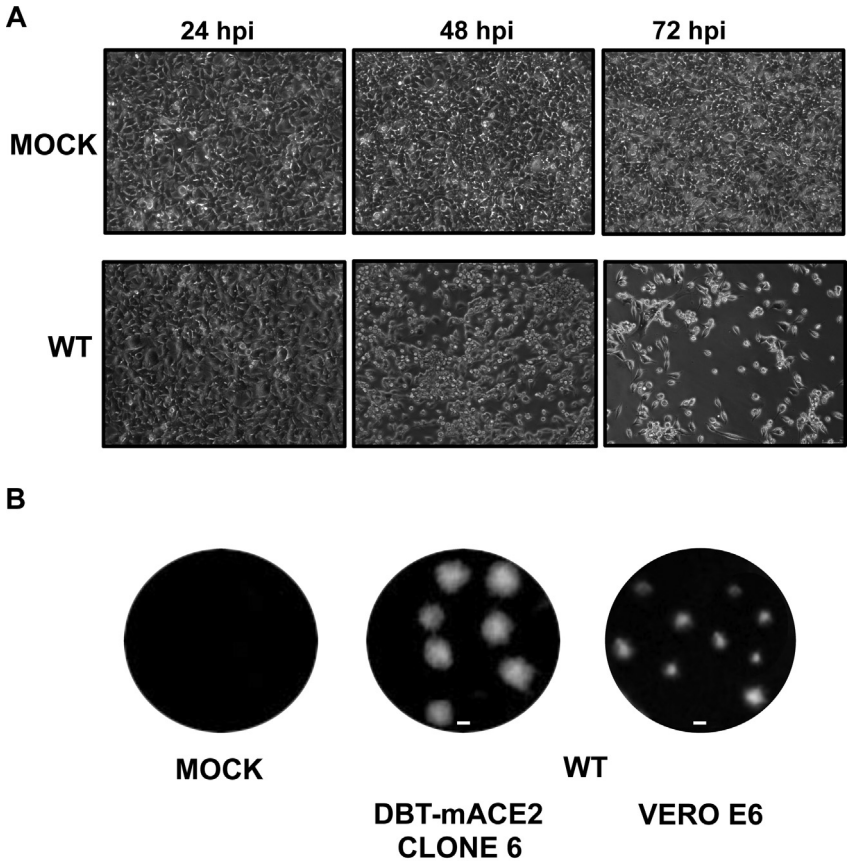

Fig. 5. Cytopathic effect and lysis plaques produced by SARS-CoV-MA15 on DBT-mACE2 clone 6 cells. (A) DBT-mACE2 clone 6 cells were mock-infected or infected with SARS-CoV-MA15 at a moi of 0.1. CPE was visualized at 24, 48, and 72 hpi. (B) Lysis plaques produced after 2 days by SARS-CoV-MA15 infection in DBT-mACE2 and Vero E6 cells.

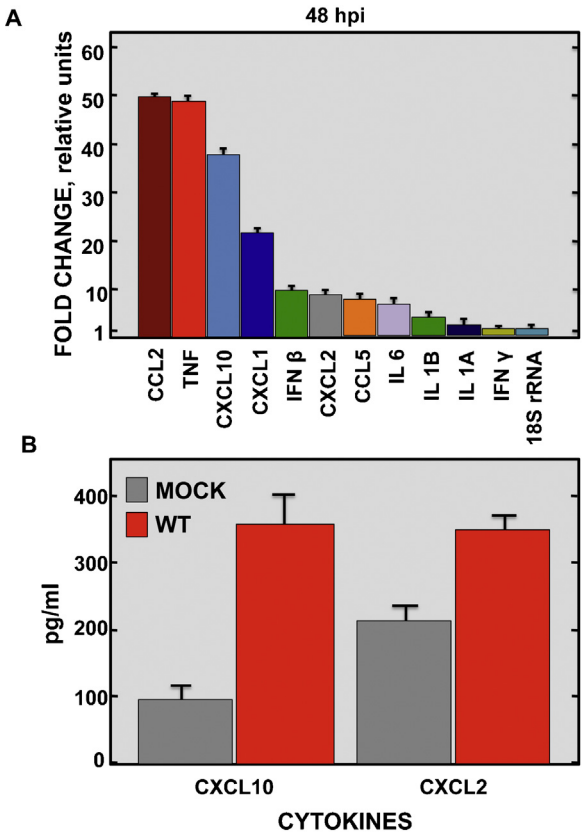

Fig. 6. Expression of proinflammatory cytokines in SARS-CoV-MA15-infected cells. DBT-mACE2 clone 6 cells were infected at a moi of 0.1 with rSARS-CoV-MA15. (A) Cellular RNAs were extracted at 48 hpi. The expression of the indicated cytokines and interferons, and that of 18S rRNA as a control, was determined by qRT-PCR. In each case, the corresponding mRNA expression levels in SARS-CoV-MA15-infected cells were plotted as fold-change relative to expression levels in uninfected cells. (B) Cell extracts were prepared at 48 hpi. Expression of the cytokines CXCL10 and CXCL2 at the protein level was evaluated in mock and DBT-mACE2-infected cells.

clear, easily identifiable plaques in DBT-mACE2 cell monolayers. Lysis plaques on DBT-mACE2 cells and Vero E6 cells were compared. Smaller plaques were observed using Vero E6 cells in comparison to DBT-mACE2 cells (Fig. 5B). Virus titers obtained by plaque assays on Vero E6 and DBT-mACE2 indicator cells were very similar (4.3×10^7 and 4.0×10^7, respectively).

3.3. Expression of inflammation related cytokines

Cytokines and IFNs are important mediators in the regulation of the immune response. To determine whether DBT-mACE2 cells are good models to evaluate the inflammatory host response to SARS-CoV infection in vitro, the mRNA expression levels of several inflammation-related cytokines and that of IFN-β and IFN-γ were analyzed by quantitative RT-PCR. Specifically, CCL2/MCP-1, tumor necrosis factor (TNF), CXCL10/IP-10, CXCL1/neutrophil activating protein 3 (NAP-3), IFN-β, CXCL2/MIP-2, CCL5/RANTES, IL6, IL1B, IL1A, and IFN-γ transcripts, and 18S rRNA, as control, were compared in both uninfected and SARS-CoV-MA15-infected cells at 24, 48 and 72 hpi. The levels of cytokine mRNAs at 24 hpi, were lower compared to 48 hpi, showing fold-increases of 1.2 to 3-fold over mock. Similar levels were observed for 48 and 72 hpi (data not shown). CCL2/MCP-1, TNF, CXCL10/IP-10 and CXCL1/NAP-3 were the most upregulated cytokines 48 h after SARS-CoV infection (between 22- and 50-fold increase; Fig. 6A). Less striking upregulations were observed for IFN-β, CXCL2/MIP-2, CCL5/RANTES and IL6, whereas more limited changes were obtained for IL 1B, IL 1A, and IFN-γ (Fig. 6A). The expression of control 18S rRNA did not change in SARS-CoV or mock-infected cells as expected (Fig. 6A).

To evaluate whether the induction of cytokine mRNAs in SARS-CoV-MA15-infected cells correlate with an induction at the protein level, the levels of CXCL10 and CXCL2 proteins were determined in mock and DBT-mACE2-infected cells. In agreement with the results obtained with the mRNAs, CXCL10 and CXCL2 were also upregulated at the protein level, showing fold-increases of 3 and 1.8-fold over mock, respectively (Fig. 6B). These data indicated that DBT-mACE2 cells were useful to study proinflammatory cytokine expression in vitro.

4. Discussion

The development of established mouse cell lines highly susceptible to mouse-adapted SARS-CoV infection is described in this study. The best current small animal model for SARS-CoV is the infection of Balb/c mice with a mouse adapted SARS-CoV (Day et al., 2009; Nagata et al., 2008; Roberts et al., 2007). The establishment of mouse cell lines susceptible to SARS-CoV was therefore of high interest, so that in vitro and in vivo evaluations with the mouse adapted SARS-CoV could take place in the same species environment and using the same cellular receptor.

The expression of mACE2 was sufficient to convert DBT cells, which were not susceptible to SARS-CoV infection, into cells producing high SARS-CoV-MA15 titers. Similarly, the transient expression of mACE2 in mouse 3T3 cells generated susceptibility to SARS-CoV infection, although these cells were not stably transformed (Li et al., 2004). In addition, the expression of civet and human ACE2 in DBT cells (Becker et al., 2008; Sheahan et al., 2008a,b), and the expression of human ACE2 in mice also led to cells susceptible to SARS-CoV and to an animal model more susceptible to the infection by a human SARS-CoV (McCray et al., 2007; Yang et al., 2007). All these data indicated that ACE2 is clearly a required SARS-CoV receptor.

SARS-CoV-Urbani titers in DBT-mACE2 cells were more than 10^3-fold lower than titers obtained for SARS-CoV-MA15. Critical mutations differentiating these two virus strains map in the gene encoding the spike protein (Roberts et al., 2007) that binds to the cellular ACE2 and facilitates virus entry (Li et al., 2003). The affinity of SARS-CoV-Urbani spike protein binding to mACE2 is lower that the affinity of SARS-CoV-MA15 spike protein binding to mACE2, making the Urbani virus entrance less efficient (Li et al., 2004).

SARS-CoV infection in DBT-mACE2 cells induced high levels of CPE, probably due to apoptosis, as it has been observed in other SARS-CoV-infected cell lines, such as Vero (DeDiego et al., 2011; Ren et al., 2005; Yan et al., 2004). This virus-induced cytopathology provides an additional experimental advantage of DBT-mACE2 cell lines, as the infection outcomes are overt and are similar to what happens to the epithelial respiratory cells in SARS patients (Lang et al., 2003; Zhang et al., 2003). Accordingly, plaque assays of SARS-CoV-MA15 were efficient in DBT-ACE2 cells.

Gene expressions leading to acute inflammation are hallmarks of SARS-CoV infection and have been associated with SARS-CoV-induced pathology (Rockx et al., 2009; Smits et al., 2010). Using genomic analysis, it has been shown that gene expressions encoding proinflammatory cytokines are increased in DBT-mACE2 cells, compared to mock-infected cells. These results correlate with the data obtained in SARS patients (Cameron et al., 2007; Huang et al., 2005; Jiang et al., 2005; Reghunathan et al., 2005; Tang et al., 2005; Wong et al., 2003; Zhang et al., 2004) and in SARS-CoV-infected monkeys and mice (Baas et al., 2008; de Lang et al., 2007; Smits et al., 2010, 2011). In addition, it has been shown that SARS-CoV-MA15 infection induced a limited IFN-β production in DBT-mACE2 cells. This weak induction could be due to the viral RNA sequestering in

double membrane vesicles described in coronaviruses (Gosert et al., 2002; Knoops et al., 2008), which prevents or reduces recognition by PRRs, and to the expression of SARS-CoV proteins that antagonize the innate response (Devaraj et al., 2007; Frieman et al., 2007; Kopecky-Bromberg et al., 2007; Narayanan et al., 2008; Siu et al., 2009; Sun et al., 2012; Wathelet et al., 2007).

The DBT-mACE2 cells generated in this work, could be used in the context of virus adaptation to a homologous receptor of another host species, such as for example hamsters or rats and in the context of mouse adaptation to the murine receptor. In addition, DBT-mACE2 cells may be useful to grow mouse adapted SARS-CoV, with reduced likelihood of undesired changes in the SARS-CoV genome that may occur during replication in non-murine cells.

Acknowledgments

This work was supported by grants from the Ministry of Science and Innovation of Spain (BIO2010-16705), the European Community's Seventh Framework Programme (FP7/2007–2013) under the project "EMPERIE" EC Grant Agreement number 223498, and U.S. National Institutes of Health (NIH) (2P01AI060699-06A1, W000306844). JAR received a fellowship from the Fundacion La Caixa. We thank Marga Gonzalez for her technical assistance.

References

Almazan, F., DeDiego, M.L., Galan, C., Escors, D., Alvarez, E., Ortego, J., Sola, I., Zuñiga, S., Alonso, S., Moreno, J.L., Nogales, A., Capiscol, C., Enjuanes, L., 2006. Construction of a SARS-CoV infectious cDNA clone and a replicon to study coronavirus RNA synthesis. Journal of Virology 80, 10900–10906.

Almazan, F., Gonzalez, J.M., Penzes, Z., Izeta, A., Calvo, E., Plana-Duran, J., Enjuanes, L., 2000. Engineering the largest RNA virus genome as an infectious bacterial artificial chromosome. Proceedings of the National Academy of Sciences of the United States of America 97, 5516–5521.

Baas, T., Roberts, A., Teal, T.H., Vogel, L., Chen, J., Tumpey, T.M., Katze, M.G., Subbarao, K., 2008. Genomic analysis reveals age-dependent innate immune responses to severe acute respiratory syndrome coronavirus. Journal of Virology 82, 9465–9476.

Becker, M.M., Graham, R.L., Donaldson, E.F., Rockx, B., Sims, A.C., Sheahan, T., Pickles, R.J., Corti, D., Johnston, R.E., Baric, R.S., Denison, M.R., 2008. Synthetic recombinant bat SARS-like coronavirus is infectious in cultured cells and in mice. Proceedings of the National Academy of Sciences of the United States of America 105, 19944–19949.

Cameron, M.J., Ran, L., Xu, L., Danesh, A., Bermejo-Martin, J.F., Cameron, C.M., Muller, M.P., Gold, W.L., Richardson, S.E., Poutanen, S.M., Willey, B.M., DeVries, M.E., Fang, Y., Seneviratne, C., Bosinger, S.E., Persad, D., Wilkinson, P., Greller, L.D., Somogyi, R., Humar, A., Keshavjee, S., Louie, M., Loeb, M.B., Brunton, J., McGeer, A.J., Kelvin, D.J., 2007. Interferon-mediated immunopathological events are associated with atypical innate and adaptive immune responses in patients with severe acute respiratory syndrome. Journal of Virology 81, 8692–8706.

Chan, P.K., To, K.F., Lo, A.W., Cheung, J.L., Chu, I., Au, F.W., Tong, J.H., Tam, J.S., Sung, J.J., Ng, H.K., 2004. Persistent infection of SARS coronavirus in colonic cells in vitro. Journal of Medical Virology 74, 1–7.

Cinatl Jr., J., Hoever, G., Morgenstern, B., Preiser, W., Vogel, J.U., Hofmann, W.K., Bauer, G., Michaelis, M., Rabenau, H.F., Doerr, H.W., 2004. Infection of cultured intestinal epithelial cells with severe acute respiratory syndrome coronavirus. Cellular and Molecular Life Sciences 61, 2100–2112.

Day, C.W., Baric, R., Cai, S.X., Frieman, M., Kumaki, Y., Morrey, J.D., Smee, D.F., Barnard, D.L., 2009. A new mouse-adapted strain of SARS-CoV as a lethal model for evaluating antiviral agents in vitro and in vivo. Virology 395, 210–222.

de Groot, R.J., Baker, S.C., Baric, R., Enjuanes, L., Gorbalenya, A.E., Holmes, K.V., Perlman, S., Poon, L., Rottier, P.J.M., Talbot, P.J., Woo, P.C.Y., Ziebuhr, J., 2012. Coronaviridae. In: King, A.M.Q., Adams, M.J., Carstens, E.B., Lefkowitz, E.J. (Eds.), Virus Taxonomy: Ninth Report of the International Committee on Taxonomy of Viruses. Elsevier Academic Press, San Diego, pp. 774–796.

de Lang, A., Baas, T., Teal, T., Leijten, L.M., Rain, B., Osterhaus, A.D., Haagmans, B.L., Katze, M.G., 2007. Functional genomics highlights differential induction of antiviral pathways in the lungs of SARS-CoV-infected macaques. PLoS Pathogens 3, e112.

DeDiego, M.L., Alvarez, E., Almazan, F., Rejas, M.T., Lamirande, E., Roberts, A., Shieh, W.J., Zaki, S.R., Subbarao, K., Enjuanes, L., 2007. A severe acute respiratory syndrome coronavirus that lacks the E gene is attenuated in vitro and in vivo. Journal of Virology 81, 1701–1713.

DeDiego, M.L., Nieto-Torres, J.L., Jimenez-Guardeno, J.M., Regla-Nava, J.A., Alvarez, E., Oliveros, J.C., Zhao, J., Fett, C., Perlman, S., Enjuanes, L., 2011. Severe acute respiratory syndrome coronavirus envelope protein regulates cell stress response and apoptosis. PLoS Pathogens 7, e1002315.

Devaraj, S.G., Wang, N., Chen, Z., Chen, Z., Tseng, M., Barretto, N., Lin, R., Peters, C.J., Tseng, C.T., Baker, S.C., Li, K., 2007. Regulation of IRF-3-dependent innate immunity by the papain-like protease domain of the severe acute respiratory syndrome coronavirus. Journal of Biological Chemistry 282, 32208–32221.

Drosten, C., Gunther, S., Preiser, W., van der Werf, S., Brodt, H.R., Becker, S., Rabenau, H., Panning, M., Kolesnikova, L., Fouchier, R.A., Berger, A., Burguiere, A.M., Cinatl, J., Eickmann, M., Escriou, N., Grywna, K., Kramme, S., Manuguerra, J.C., Muller, S., Rickerts, V., Sturmer, M., Vieth, S., Klenk, H.D., Osterhaus, A.D., Schmitz, H., Doerr, H.W., 2003. Identification of a novel coronavirus in patients with severe acute respiratory syndrome. New England Journal of Medicine 348, 1967–1976.

Enjuanes, L., Gorbalenya, A.E., de Groot, R.J., Cowley, J.A., Ziebuhr, J., Snijder, E.J., 2008. The nidovirales. In: Mahy, B.W.J., Van Regenmortel, M., Walker, P., Majumder-Russell, D. (Eds.), Encyclopedia of Virology, 3rd ed. Elsevier Ltd., Oxford, pp. 419–430.

Fett, C., DeDiego, M.L., Regla-Nava, J.A., Enjuanes, L., Perlman, S., 2013. Complete protection against severe acute respiratory syndrome coronavirus-mediated lethal respiratory disease in aged mice by immunization with a mouse-adapted virus lacking E protein. Journal of Virology 87, 6551–6559.

Fouchier, R.A., Kuiken, T., Schutten, M., van Amerongen, G., van Doornum, G.J., van den Hoogen, B.G., Peiris, M., Lim, W., Stohr, K., Osterhaus, A.D., 2003. Aetiology: Koch's postulates fulfilled for SARS virus. Nature 423, 240.

Frieman, M., Heise, M., Baric, R., 2008. SARS coronavirus and innate immunity. Virus Research 133, 101–112.

Frieman, M., Yount, B., Heise, M., Kopecky-Bromberg, S.A., Palese, P., Baric, R.S., 2007. Severe acute respiratory syndrome coronavirus ORF6 antagonizes STAT1 function by sequestering nuclear import factors on the rough endoplasmic reticulum/Golgi membrane. Journal of Virology 81, 9812–9824.

Gallagher, T.M., Buchmeier, M.J., 2001. Coronavirus spike proteins in viral entry and pathogenesis. Virology 279, 371–374.

Gosert, R., Kanjanahaluethai, A., Egger, D., Bienz, K., Baker, S.C., 2002. RNA replication of mouse hepatitis virus takes place at double-membrane vesicles. Journal of Virology 76, 3697–3708.

Hattermann, K., Muller, M.A., Nitsche, A., Wendt, S., Donoso Mantke, O., Niedrig, M., 2005. Susceptibility of different eukaryotic cell lines to SARS-coronavirus. Archives of Virology 150, 1023–1031.

Huang, K.J., Su, I.J., Theron, M., Wu, Y.C., Lai, S.K., Liu, C.C., Lei, H.Y., 2005. An interferon-gamma-related cytokine storm in SARS patients. Journal of Medical Virology 75, 185–194.

Jeffers, S.A., Tusell, S.M., Gillim-Ross, L., Hemmila, E.M., Achenbach, J.E., Babcock, G.J., Thomas Jr., W.D., Thackray, L.B., Young, M.D., Mason, R.J., Ambrosino, D.M., Wentworth, D.E., Demartini, J.C., Holmes, K.V., 2004. CD209L (L-SIGN) is a receptor for severe acute respiratory syndrome coronavirus. Proceedings of the National Academy of Sciences of the United States of America 101, 15748–15753.

Jiang, Y., Xu, J., Zhou, C., Wu, Z., Zhong, S., Liu, J., Luo, W., Chen, T., Qin, Q., Deng, P., 2005. Characterization of cytokine/chemokine profiles of severe acute respiratory syndrome. American Journal of Respiratory and Critical Care Medicine 171, 850–857.

Knoops, K., Kikkert, M., Worm, S.H., Zevenhoven-Dobbe, J.C., van der Meer, Y., Koster, A.J., Mommaas, A.M., Snijder, E.J., 2008. SARS-coronavirus replication is supported by a reticulovesicular network of modified endoplasmic reticulum. PLoS Biology 6, e226.

Kopecky-Bromberg, S.A., Martinez-Sobrido, L., Frieman, M., Baric, R.A., Palese, P., 2007. Severe acute respiratory syndrome coronavirus open reading frame (ORF) 3b, ORF 6, and nucleocapsid proteins function as interferon antagonists. Journal of Virology 81, 548–557.

Ksiazek, T.G., Erdman, D., Goldsmith, C., Zaki, S., Peret, T., Emery, S., Tong, S., Urbani, C., Comer, J.A., Lim, W., Rollin, P.E., Dowell, S., Ling, A.-E., Humphrey, C., Shieh, W.-J., Guarner, J., Paddock, C.D., Rota, P., Fields, B., DeRisi, J., Yang, J.-Y., Cox, N., Hughes, J., LeDuc, J.W., Bellini, W.J., Anderson, L.J., 2003. A novel coronavirus associated with severe acute respiratory syndrome. New England Journal of Medicine 348, 1953–1966.

Kuiken, T., Fouchier, R.A.M., Schutten, M., Rimmelzwaan, G.F., van Amerongen, G., van Riel, D., Laman, J.D., de Jong, T., van Doornum, G., Lim, W., Ling, A.E., Chan, P.K.S., Tam, J.S., Zambon, M.C., Gopal, R., Drosten, C., van der Werf, S., Escriou, N., Manuguerra, J.-C., Stohr, K., Peiris, J.S.M., 2003. Newly discovered coronavirus as the primary cause of severe acute respiratory syndrome. Lancet 362, 263–270.

Kumanishi, T., 1967. Brain tumors induced with Rous sarcoma virus, Schmidt-Ruppin strain. I. Induction of brain tumors in adult mice with Rous chicken sarcoma cells. Japanese Journal of Experimental Medicine 37, 461–474.

Lang, Z.W., Zhang, L.J., Zhang, S.J., Meng, X., Li, J.Q., Song, C.Z., Sun, L., Zhou, Y.S., Dwyer, D.E., 2003. A clinicopathological study of three cases of severe acute respiratory syndrome (SARS). Pathology 35, 526–531.

Lau, S.K., Woo, P.C., Li, K.S., Huang, Y., Tsoi, H.W., Wong, B.H., Wong, S.S., Leung, S.Y., Chan, K.H., Yuen, K.Y., 2005. Severe acute respiratory syndrome coronavirus-like virus in Chinese horseshoe bats. Proceedings of the National Academy of Sciences of the United States of America 102, 14040–14045.

Li, F., Li, W., Farzan, M., Harrison, S.C., 2005. Structure of SARS coronavirus spike receptor-binding domain complexed with receptor. Science 309, 1864–1868.

Li, W., Greenough, T.C., Moore, M.J., Vasilieva, N., Somasundaran, M., Sullivan, J.L., Farzan, M., Choe, H., 2004. Efficient replication of severe acute respiratory syndrome coronavirus in mouse cells is limited by murine angiotensin-converting enzyme 2. Journal of Virology 78, 11429–11433.

Li, W., Moore, M.J., Vasilieva, N., Sui, J., Wong, S.K., Berne, M.A., Somasundaran, M., Sullivan, J.L., Luzuriaga, K., Greenough, T.C., Choe, H., Farzan, M., 2003. Angiotensin-converting enzyme 2 is a functional receptor for de SARS coronavirus. Nature 426, 450–454.

Livak, K.J., Schmittgen, T.D., 2001. Analysis of relative gene expression data using real-time quantitative PCR and the 2(-Delta Delta C(T)) Method. Methods 25, 402–408.

Marra, M.A., Jones, S.J.M., Astell, C.R., Holt, R.A., Brooks-Wilson, A., Butterfield, Y.S.N., Khattra, J., Asano, J.K., Barber, S.A., Chan, S.Y., Cloutier, A., Coughlin, S.M., Freeman, D., Girn, N., Griffith, O.L., Leach, S.R., Mayo, M., McDonald, H., Montgomery, S.B., Pandoh, P.K., Petrescu, A.S., Robertson, A.G., Schein, J.E., Siddiqui, A., Smailus, D.E., Stott, J.M., Yang, G.S., Plummer, F., Andonov, A., Artsob, H., Bastien, N., Bernard, K., Booth, T.F., Bowness, D., Czub, M., Drebot, M., Fernando, L., Flick, R., Garbutt, M., Gray, M., Grolla, A., Jones, S., Feldmann, H., Meyers, A., Kabani, A., Li, Y., Normand, S., Stroher, U., Tipples, G.A., Tyler, S., Vogrig, R., Ward, D., Watson, B., Brunham, R.C., Krajden, M., Petric, M., Skowronski, D.M., Upton, C., Roper, R.L., 2003. The genome sequence of the SARS-associated coronavirus. Science 300, 1399–1404.

McCray Jr., P.B., Pewe, L., Wohlford-Lenane, C., Hickey, M., Manzel, L., Shi, L., Netland, J., Jia, H.P., Halabi, C., Sigmund, C.D., Meyerholz, D.K., Kirby, P., Look, D.C., Perlman, S., 2007. Lethal infection of K18-hACE2 mice infected with severe acute respiratory syndrome coronavirus. Journal of Virology 81, 813–821.

Mossel, E.C., Huang, C., Narayanan, K., Makino, S., Tesh, R.B., Peters, C.J., 2005. Exogenous ACE2 expression allows refractory cell lines to support severe acute respiratory syndrome coronavirus replication. Journal of Virology 79, 3846–3850.

Nagata, N., Iwata, N., Hasegawa, H., Fukushi, S., Harashima, A., Sato, Y., Saijo, M., Taguchi, F., Morikawa, S., Sata, T., 2008. Mouse-passaged severe acute respiratory syndrome-associated coronavirus leads to lethal pulmonary edema and diffuse alveolar damage in adult but not young mice. American Journal of Pathology 172, 1625–1637.

Narayanan, K., Huang, C., Lokugamage, K., Kamitani, W., Ikegami, T., Tseng, C.T., Makino, S., 2008. Severe acute respiratory syndrome coronavirus nsp1 suppresses host gene expression, including that of type I interferon, in infected cells. Journal of Virology 82, 4471–4479.

Ng, M.L., Tan, S.H., See, E.E., Ooi, E.E., Ling, A.E., 2003. Proliferative growth of SARS coronavirus in Vero E6 cells. Journal of General Virology 84, 3291–3303.

Peiris, J.S.M., Lai, S.T., Poon, L.L.M., Guan, Y., Yam, L.Y.C., Lim, W., Nicholls, J., Yee, W.K.S., Yan, W.W., Cheung, M.T., 2003. Coronavirus as a possible cause of severe acute respiratory syndrome. Lancet 361, 1319–1325.

Reghunathan, R., Jayapal, M., Hsu, L.Y., Chng, H.H., Tai, D., Leung, B.P., Melendez, A.J., 2005. Expression profile of immune response genes in patients with Severe Acute Respiratory Syndrome. BMC Immunology 6, 2.

Ren, L., Yang, R., Guo, L., Qu, J., Wang, J., Hung, T., 2005. Apoptosis induced by the SARS-associated coronavirus in Vero cells is replication-dependent and involves caspase. DNA and Cell Biology 24, 496–502.

Roberts, A., Deming, D., Paddock, C.D., Cheng, A., Yount, B., Vogel, L., Herman, B.D., Sheahan, T., Heise, M., Genrich, G.L., Zaki, S.R., Baric, R., Subbarao, K., 2007. A mouse-adapted SARS-coronavirus causes disease and mortality in BALB/c mice. PLoS Pathogens 3, 23–37.

Roberts, A., Lamirande, E.W., Vogel, L., Jackson, J.P., Paddock, C.D., Guarner, J., Zaki, S.R., Sheahan, T., Baric, R., Subbarao, K., 2008. Animal models and vaccines for SARS-CoV infection. Virus Research 133, 20–32.

Rockx, B., Baas, T., Zornetzer, G.A., Haagmans, B., Sheahan, T., Frieman, M., Dyer, M.D., Teal, T.H., Proll, S., van den Brand, J., Baric, R., Katze, M.G., 2009. Early upregulation of acute respiratory distress syndrome-associated cytokines promotes lethal disease in an aged-mouse model of severe acute respiratory syndrome coronavirus infection. Journal of Virology 83, 7062–7074.

Rota, P.A., Oberste, M.S., Monroe, S.S., Nix, W.A., Campganoli, R., Icenogle, J.P., Peñaranda, S., Bankamp, B., Maher, K., Chen, M.-H., Tong, S., Tamin, A., Lowe, L., Frace, M., DeRisi, J.L., Chen, Q., Wang, D., Erdman, D.d., Peret, T.C.T., Burns, C., Ksiazek, T.G., Rollin, P.E., Sanchez, A., Liffick, S., Holloway, B., Limor, J., McCaustland, K., Olsen-Rassmussen, M., Fouchier, R., Gunther, S., Osterhaus, A.D.M.E., Drosten, C., Pallansch, M.A., Anderson, L.J., Bellini, W.J., 2003. Characterization of a novel coronavirus associated with severe acute respiratory syndrome. Science 300, 1394–1399.

Sheahan, T., Rockx, B., Donaldson, E., Corti, D., Baric, R., 2008a. Pathways of cross-species transmission of synthetically reconstructed zoonotic severe acute respiratory syndrome coronavirus. Journal of Virology 82, 8721–8732.

Sheahan, T., Rockx, B., Donaldson, E., Sims, A., Pickles, R., Corti, D., Baric, R., 2008b. Mechanisms of zoonotic severe acute respiratory syndrome coronavirus host range expansion in human airway epithelium. Journal of Virology 82, 2274–2285.

Siu, K.L., Kok, K.H., Ng, M.H., Poon, V.K., Yuen, K.Y., Zheng, B.J., Jin, D.Y., 2009. Severe acute respiratory syndrome coronavirus M protein inhibits type I interferon production by impeding the formation of TRAF3.TANK.TBK1/IKKepsilon complex. Journal of Biological Chemistry 284, 16202–16209.

Smits, S.L., de Lang, A., van den Brand, J.M., Leijten, L.M., van, I.W.F., Eijkemans, M.J., van Amerongen, G., Kuiken, T., Andeweg, A.C., Osterhaus, A.D., Haagmans, B.L., 2010. Exacerbated innate host response to SARS-CoV in aged non-human primates. PLoS Pathogens 6, e1000756.

Smits, S.L., van den Brand, J.M., de Lang, A., Leijten, L.M., van Ijcken, W.F., van Amerongen, G., Osterhaus, A.D., Andeweg, A.C., Haagmans, B.L., 2011. Distinct severe acute respiratory syndrome coronavirus-induced acute lung injury pathways in two different nonhuman primate species. Journal of Virology 85, 4234–4245.

Subbarao, K., Roberts, A., 2006. Is there an ideal animal model for SARS? Trends in Microbiology 14, 299–303.

Sun, L., Xing, Y., Chen, X., Zheng, Y., Yang, Y., Nichols, D.B., Clementz, M.A., Banach, B.S., Li, K., Baker, S.C., Chen, Z., 2012. Coronavirus papain-like proteases negatively regulate antiviral innate immune response through disruption of STING-mediated signaling. PloS ONE 7, e30802.

Tang, N.L., Chan, P.K., Wong, C.K., To, K.F., Wu, A.K., Sung, Y.M., Hui, D.S., Sung, J.J., Lam, C.W., 2005. Early enhanced expression of interferon-inducible protein-10 (CXCL-10) and other chemokines predicts adverse outcome in severe acute respiratory syndrome. Clinical Chemistry 51, 2333–2340.

Wathelet, M.G., Orr, M., Frieman, M.B., Baric, R.S., 2007. Severe acute respiratory syndrome coronavirus evades antiviral signaling: role of nsp1 and rational design of an attenuated strain. Journal of Virology 81, 11620–11633.

Wong, R.S., Wu, A., To, K.F., Lee, N., Lam, C.W., Wong, C.K., Chan, P.K., Ng, M.H., Yu, L.M., Hui, D.S., Tam, J.S., Cheng, G., Sung, J.J., 2003. Haematological manifestations in patients with severe acute respiratory syndrome: retrospective analysis. BMJ 326, 1358–1362.

Wong, S.K., Li, W., Moore, M.J., Choe, H., Farzan, M., 2004. A 193-amino acid fragment of the SARS coronavirus S protein efficiently binds angiotensin-converting enzyme 2. Journal of Biological Chemistry 279, 3197–3201.

Woo, P.C., Lau, S.K., Li, K.S., Poon, R.W., Wong, B.H., Tsoi, H.W., Yip, B.C., Huang, Y., Chan, K.H., Yuen, K.Y., 2006. Molecular diversity of coronaviruses in bats. Virology 351, 180–187.

Yan, H., Xiao, G., Zhang, J., Hu, Y., Yuan, F., Cole, D.K., Zheng, C., Gao, G.F., 2004. SARS coronavirus induces apoptosis in Vero E6 cells. Journal of Medical Virology 73, 323–331.

Yang, X.H., Deng, W., Tong, Z., Liu, Y.X., Zhang, L.F., Zhu, H., Gao, H., Huang, L., Liu, Y.L., Ma, C.M., Xu, Y.F., Ding, M.X., Deng, H.K., Qin, C., 2007. Mice transgenic for human angiotensin-converting enzyme 2 provide a model for SARS coronavirus infection. Comparative Medicine 57, 450–459.

Zhang, Q.L., Ding, Y.Q., He, L., Wang, W., Zhang, J.H., Wang, H.J., Cai, J.J., Geng, J., Lu, Y.D., Luo, Y.L., 2003. Detection of cell apoptosis in the pathological tissues of patients with SARS and its significance. Di Yi Jun Yi Da Xue Xue Bao 23, 770–773.

Zhang, Y., Li, J., Zhan, Y., Wu, L., Yu, X., Zhang, W., Ye, L., Xu, S., Sun, R., Wang, Y., Lou, J., 2004. Analysis of serum cytokines in patients with severe acute respiratory syndrome. Infection and Immunity 72, 4410–4415.

Ziebuhr, J., Snijder, E.J., Gorbalenya, A.E., 2000. Virus-encoded proteinases and proteolytic processing in the *Nidovirales*. Journal of General Virology 81, 853–879.